

Identification of 13 independent genetic loci associated with cognitive resilience in healthy aging in 330,097 individuals in the UK Biobank.

Joan Fitzgerald¹, Laura Fahey^{1,2}, Laurena Holleran¹, Pilib Ó Broin², Gary Donohoe¹, Derek W. Morris¹

¹ Cognitive Genetics and Cognitive Therapy Group, Centre for Neuroimaging & Cognitive Genomics, School of Psychology and Discipline of Biochemistry, National University of Ireland Galway, Galway, Ireland.

² School of Mathematics, Statistics and Applied Mathematics, National University of Ireland Galway, Galway, Ireland.

Corresponding author:

Dr Derek Morris, Room 106, Discipline of Biochemistry, National University of Ireland Galway,

University Road, Galway, Ireland.

Tel: + 353 91 494439; Email: derek.morris@nuigalway.ie

Abstract

Cognitive resilience is the ability to withstand the negative effects of stress on cognitive functioning and is important for maintaining quality of life while aging. Here we employed a proxy phenotype approach to create a longitudinal cognitive resilience phenotype using past education years and current processing speed, reflecting an average time span of 40 years, in 330,097 individuals from the UK Biobank. A genome-wide association study identified 13 independent genome-wide significant loci that implicate 33 genes. A portion of resilience's genetic signal is distinct from the genetics of intelligence. Functional analyses showed enrichment in several brain regions and involvement of specific cell types, including GABAergic neurons ($P=6.59 \times 10^{-8}$) and glutamatergic neurons ($P=6.98 \times 10^{-6}$) in the cortex. Gene-set analyses implicated the biological process "neuron differentiation" ($P=9.7 \times 10^{-7}$) and the cellular component "synaptic part" ($P=2.14 \times 10^{-6}$). Mendelian randomization analysis showed a causative effect of white matter volume on cognitive resilience. These results enhance neurobiological understanding of resilience.

Introduction:

Cognitive decline is one of the most feared aspects of aging leading to major health and social issues and is associated with illness, dementia and death [1]. Non-pathological or age-related cognitive decline leads to increased challenges in completing tasks that require information processing and memory, which in turn leads to a deleterious effect on an individual's enjoyment of and participation in life events [2]. Cognitive resilience is our ability to withstand negative effects of stress and maintain cognitive functioning. Understanding the factors that contribute to resilience is becoming increasingly important given the aging demographics of the world's population [3]. There is a growing knowledge of how non-genetic factors such as cardiovascular health and social participation contribute to cognitive resilience [4]; however an understanding of the genetic contribution has been hampered by the lack of large datasets with genetic data and suitable longitudinal data on cognition.

One theory that examines the biological influences on rates of cognitive decline in healthy aging is the concept of reserve, maintenance, and compensation leading to cognitive resilience[5]. Reserve is usually described in terms of both brain reserve, which is the overall strength of size of structural components such as quantity of neurons and synapses and cognitive reserve, which refers to adaptability of these components [6]. These are hypothesised to reflect a level of neural resources built up over our lifetime, maintained via the ability to repair cellular damage to maintain cognitive function, with losses compensated for by use of alternative undamaged cognitive functions. In turn these mechanisms are thought to be mediated by a combination of environmental and genetic factors.

Others propose that variation in the rate of cognitive decline can be explained by variation in intelligence. Longitudinal analysis in the Lothian Birth Cohort has shown that childhood intelligence has a protective effect on cognitive decline in late life [7]. Other studies show that while higher education reflects greater cognitive ability, the rates of change in that ability over time are consistent across all education levels, with those starting at a higher level simply having further to fall before they present with mild cognitive impairment [8] [9]. The role of intelligence is confounded by the fact that higher intelligence is associated with healthier life styles, which has a protective effect on cognitive decline [10].

The purpose of this study was to explore genetic variation associated with cognitive resilience within the UK Biobank (UKB) [11]. In the absence of direct measurements of

cognitive ability at distal timepoints we employed proxy phenotypes. We used number of years in education (education years (EY)) as a proxy phenotype for cognitive performance in early adulthood, following several previous studies [12-14]. Current cognitive performance was determined based on reaction time (RT) as a measure of processing speed. This approach captures an average time span of 40 years between past and current cognitive performance in UKB. A confounding factor in this strategy is that EY is highly heritability with a polygenic nature [15] that can mask the genetics of resilience. To overcome this we employed Genomics Structural Equation Modelling (GenomicSEM) [16] to perform a GWAS-by-subtraction [17] using two GWAS, one which captured genetic variants associated with EY and resilience and a second which captured genetic variants associated with EY but not resilience. Subtracting one from the other generated two new GWAS, one capturing EY and the other capturing the genetics of resilience. Replication of this approach was shown using independent discovery and replication samples and the full GWAS results were examined further using functional genomics analysis. We found 13 independent genetic loci for resilience. Extensive functional *in silico* analyses showed the involvement of specific tissue and cell types. Resilience is genetically correlated with multiple cognitive phenotypes, brain disorders and measures of brain volume. Mendelian randomization identified causal effects of white matter volume on resilience.

Results:

Initial phenotype development

Figure 1 shows an overview of the analysis steps and a detailed description of the process used to generate the resilience variable is included in the online methods. Given the multi-step method proposed in this analysis, we sought confirm findings using our method in an independent sample. Therefore, we divided the UKB into discovery (n=266,543; 81% of participants) and replication (n=63,554; 19% of participants) samples (Figure 1a). Sample sizes used for analysis are shown in Supplementary Table 1. We used EY as a proxy phenotype measuring past cognitive performance [13]. EY was calculated using a combination of data supplied on years in education and educational attainment (see online methods). Processing speed as measured by RT was chosen as an indicator of current cognitive performance given its strong correlation with age and the fact that data was available on most participants in UKB. We created a binary variable for each measure by using the average score within the dataset to split the participants into similarly sized groups. EY was split into above and below average based on participants completing greater than or equal to 17 years, or less than 17 years in education. RT was split into faster and slower based on participants having a processing speed better or worse than the mean value (see online methods), such that faster RT speeds reflected better cognitive performance than slower RT. By combining these two binary variables, we created four groups of participants (Figure 1b). One of these groups demonstrated high resilience and these were our cases for GWAS who had below average EY previously and faster than average RT now. A second group demonstrated low resilience or cognitive decline, and these were our controls for GWAS who had above average EY previously and slower than average RT now. Results for this GWAS were dominated by SNPs associated with EY because the high resilience cases and low resilience controls had below average and above average EY measures, respectively. We named this GWAS “EY+Res” because it identified SNPs associated with both EY and resilience (Figure 1c).

In order to identify those SNPs that were associated with resilience alone and remove those SNPs that were associated with the EY component of the phenotype, we performed a second GWAS using the two remaining groups of UKB samples that displayed consistent (i.e. unchanging) cognitive performance over time. The first of these groups consisted of those with below average EY previously and slower than average RT now (i.e. consistently below

average cognition over time); the second group consisted of those who showed above average EY previously and faster than average RT now (i.e. consistently above average cognition over time). We named this GWAS “EY/NonRes” because it identified SNPs associated with EY but not resilience (Figure 1d).

We then used GWAS-by-subtraction (GBS) [17] to subtract the results of EY/NonRes from EY+Res to leave SNP associations with resilience. This method uses GenomicSEM [16] to integrate GWAS into structural equation modelling. Following the process described by Demange et al [17], we defined a Cholesky model (Figure 2) using the summary statistics from the EY+Res and EY/NonRes GWASs. Both EY+Res and EY/NonRes were regressed on a latent factor, which captured the shared genetic variance in EY (hereafter “*EduYears*”). EY+Res was further regressed on a second latent factor capturing the variance in EY+Res independent of EY/NonRes, hereafter “*Resilience*”. Genetic variance in *Resilience* was independent of genetic variance in *EduYears* ($r_g=0$) as the *Resilience* factor represents residual genetic variation in our EY+Res phenotype that is not accounted for by the *EduYears* factor. These two latent variables, *Resilience* and *EduYears* were then regressed on each SNP in the original GWASs (EY+Res and EY/NonRes) resulting in new GWAS summary statistics for both *Resilience* and *EduYears* (Figure 1e).

Discovery and replication analysis

For the discovery sample, we performed the two initial GWASs (discovery.EY+Res and discovery.EY/NonRes) and then performed GBS on both sets of samples resulting in *discovery.Resilience* GWAS results and *discovery.EduYears* GWAS results. We repeated this for the replication sample to produce *replication.Resilience* GWAS results and *replication.EduYears* GWAS results. Comparison of the *discovery.Resilience* GWAS with the *replication.Resilience* GWAS by LD score regression (LDSR) analysis [16] showed extremely high correlation between the two data sets ($r_g = 0.964$, $P = 4.45 \times 10^{-44}$). The *discovery.Resilience* GWAS was then processed through FUMA v 1.3.6 [18] and ten independent genome-wide significant SNPs were identified. When compared to the *replication.Resilience* GWAS, there was a consistent direction of effect for all ten SNPs (Binomial sign test, $P = 9.77 \times 10^{-4}$). Five of the ten SNPs were significant after Bonferroni multiple test correction for those SNPs tested ($P < 0.005$). Thus, we demonstrated that we could replicate genetic associations with *Resilience* in an independent sample. Results for the ten-independent genome-wide significant SNPs and their replication analysis are in Supplementary Table 2.

Analysis of the full sample

Next, we combined both the discovery and replication samples to run an analysis on the full sample ($n=330,097$). This resulted in initial EY+Res and EY/NonRes GWASs and following GBS, *Resilience* GWAS results and *EduYears* GWAS results. SNP based heritability estimate analysis showed a h^2 value of 0.13 ($SE = .006$) for *Resilience*. For comparison in similarly sized samples, we also ran GWASs of EY and RT using participants randomly selected from UKB (EY, $n=82,000$ above average EY cases and $n=81,999$ below average EY controls; RT, $n=82,000$ faster than average RT cases and $n=82,000$ slower than average RT controls). A Manhattan plot and a Quantile-quantile (Q-Q) plot of *Resilience* on the full sample is shown in Figure 3a and 3b. Manhattan plots for the other five GWAS (EY+Res, EY/NonRes, *EduYears*, EY and RT) are in Supplementary Figure 1.

Initially, both EY+Res and EY/NonRes had a strong negative correlation with EY ($r_g = -0.88$ and $r_g = -0.89$ respectively (Supplementary Figure 2)). The strength of these correlations likely reflect the major contribution of EY to these phenotypes and they are negative because for EY+Res and EY/NonRes, the direction of effect is in the opposite direction to EY, as the cases are low EY whereas for the EY GWAS, the cases are high EY. EY+Res and EY/NonRes had a moderate positive correlation with each other ($r_g = 0.54$). After GBS there was no genetic correlation between *Resilience* and *EduYears* ($r_g = 0.01$, $P = 0.803$) suggesting that the subtraction had successfully separated out the genetic associations for both phenotypes.

Although the EY component of *Resilience* was addressed by the GBS method, the RT component was not and the genetic correlation between *Resilience* and RT was strong ($r_g = 0.80$; Supplementary Figure 2). One possible concern was that we were just identifying genetic associations with RT that are independent of EY. However, when we compared results for the 13 index SNPs in the *Resilience* GWAS across the six GWAS including RT as a stand-alone phenotype only one of the 13 SNPs was itself genome-wide significant for RT and just three others were associated at $P < 1 \times 10^{-4}$ (Supplementary Table 3). The genetic correlation between *Resilience* and RT is strong because this is an RT-based resilience phenotype; however, the top associated SNPs for RT were not being detected here. Instead, we detected SNPs associated with faster than average RT in individuals that previously showed below average EY, i.e., the resilience phenotype in this study.

Functional analysis

Description of genetic loci

Function analysis was performed on *Resilience* in FUMA v 1.3.6 [18]. (Note: see Online Methods for parameters used and results publicly available in FUMA ID:171).

A total of 1,329 significant SNPs were tagged from the *Resilience* GWAS and were associated with 26 independent lead SNPs ($P < 5 \times 10^{-8}$). Including SNPs in the reference panel that are in LD with the independent SNPs, resulted in a total of 1,922 candidate SNPs. Functional annotation of the candidate SNPs showed that 82% were intergenic/intronic. A total of 84 SNPs had a Combined Annotation Dependent Depletion (CADD) score greater than the threshold of 12.37 which indicates that the variation is potentially pathogenic [19] (see Supplementary Table 4 and 5).

Lead SNPs were grouped into 13 independent genetic loci which are on 9 chromosomes. Detailed maps of each locus are available in Supplementary Figure 3. Conditional analyses showed that the significance of all independent lead SNPs at each locus was reduced when the GWAS was conditioned for the index or most associated SNP, confirming the linkage of the index SNP to each lead SNP (Supplementary Table 6).

Fine Mapping

FINEMAP [20] was used to provide further information on significant SNPs in LD with the index SNP on each locus using the GWAS SNPs generated by FUMA (Supplementary Table 7). The \log_{10} Bayes factor (B_{10}) quantifies causal evidence for a particular SNP and a posterior probability value yielding a B_{10} greater than 2 indicates considerable evidence of causality [20]. One SNP, rs62074125, on chromosome 17, exceeded this value ($B_{10} = 2.64$). This SNP is an intron within the *WNT3* gene, which is associated with cognitive function [21]. The next highest result was on chromosome 4 where rs2189234 had a value slightly below 2 ($B_{10} = 1.62$). This SNP is an intronic variant in the *TET2* gene, which is discussed below. FINEMAP analysis showed that the index SNP had the highest Bayes Factor for all loci with four exceptions (Supplementary Table 8).

Gene mapping

Three approaches were used in FUMA to map the associated variants to genes: (a) Positional mapping that mapped 141 SNPs to genes based on their genomic location within a 10 kilobase window of known gene boundaries. (b) Expression quantitative trait (eQTL) mapping that mapped 207 cis-eQTL SNPs to genes whose expression they affected. (c) Chromatin interaction mapping using the 3D DNA to DNA interactions that mapped SNPs to 243 genes. Circos plots for all loci are included in Supplementary Figure 4. The circos plot from chromosome 3 shows that 102 genes were mapped to this region, representing 42% of the total genes mapped. In addition, the circos plot from chromosome 17 shows two distinct clusters of SNPs. Genes in this region (*MAPT*, *WNT3*, *CRHRI*, *KANSL1*, and *NSF*) have been previously associated with general cognitive function but also with other cognitive indicators [21]. Details of this gene mapping analysis is in Supplementary Table 9.

In addition to the three approaches above we also performed a genome-wide gene-based association analysis (GWGAS) using the MAGMA function within FUMA [18], which looks at the aggregate association results of all SNPs in a gene in contrast to the previous analyses that examined the association signals at the level of individual SNPs. A GWGAS was performed using the *Resilience* GWAS on 18,879 protein-coding genes containing at least one SNP from the GWAS. Based on the number of genes tested, a Bonferroni-corrected threshold of $P < 2.65 \times 10^{-6}$ was used (see Q-Q plot of this association – figure 3c). A total of 52 protein coding genes were identified as associated, 40 of which were identified by the previously described strategies (Supplementary Table 10). In total, 33 genes were identified by all four mapping strategies (Figure 3c and Supplementary Table 11).

Many of these 33 genes have been connected with cognitive performance, neurodegenerative disorders or aging and represent potential therapeutic targets: *STAU1* (chr 20) and *SEMA3F* (chr 3) are predicted to control cognitive decline in aging through formation of neural circuits and synaptic transmission [22]. *BNS* (chr 3) codes for bassoon presynaptic cytomatrix protein which is implicated in the regulation of neurotransmitters at inhibitory and excitatory synapses [23]. *IP6KI* (chr 3) codes for inositol pyrophosphate biosynthesis, and mouse studies have shown its involvement in short term memory by altering presynaptic vesicle release and short-term facilitation of glutamatergic synapses in the hippocampus [24]. *MST1* (chr 3) has been shown to play a role in protecting cells from oxidative stress which leads to

aging and eventual cell death [25]. *TET2* (chr 4) codes for ten eleven translocation methyl cytosine dioxygenase 2 which catalyses the production of 5-hydroxymethylcytosine and is associated with increased neurogenesis in the hippocampus and cognition in animal studies [26]. *ATXN2* (chr 20) is involved in regulating mRNA and is linked to decline in cognitive function in older adults [27], general cognitive function [21] and neurodegenerative disorders [28]. The *ATXN2/BRAP* locus has a strong association with parenteral lifespan [29]. Another mapped gene close to *ATXN2* and *BRAP* is *SH2B3*, which encodes lymphocyte adaptor protein LNK, and plays a role in human aging though the mechanism involved is not fully understood [30]. The gene *ALDH2* (chr 12) codes for aldehyde dehydrogenase and there is a link between this enzyme and life span as well as cardiovascular aging [31].

Among the associated SNPs at the 33 prioritized genes are two UTR3 variants on chromosome 3 (rs2681781 (CADD=17.77) and rs4625 (CADD=15.6)) that map to *RBM5* and *DAG1* respectively. Animal studies have shown that *RBM5* is a likely regulator of Rab4a, which is involved in many neurobiological functions including the transport of transmembrane proteins required for neurotransmission [32]. *DAG1* has been associated with increased cognitive performance and is associated with GABAergic signalling in the hippocampus [33]. In addition, one other variant of note is rs1130146 that maps to *DDX27* (chr 20), a gene that was mapped by all strategies except for GWAS and is associated with longevity [34]. This missense SNP has a CADD score of 31 and is predicted by SIFT to be deleterious and by PolyPhen to be possibly damaging.

Tissue, cell type and pathway enrichment analysis

Using gene expression data for 53 tissues obtained from GTEx [35], we found all brain regions to be significantly enriched for our associated genes with the strongest enrichments for the frontal cortex, BA9 ($P = 2.26 \times 10^{-11}$), the cortex ($P = 8.48 \times 10^{-11}$) and the cerebellar hemisphere ($P = 1.18 \times 10^{-10}$; Figure 4a and Supplementary Table 12). There was no significant enrichment in other tissues of the body. Expression analysis at the cellular level was performed using data sets from the Human Prefrontal cortex by age [36], the Human Cortex [37] and Linnarsson Mouse Brain Atlas [38]. We analysed significant cell types across datasets, independent cell type associations based on within-dataset conditional analyses and pair-wise cross-datasets conditional analyses (Figure 4b and Supplementary Tables 13 and 14). These analyses identified four neuronal cell types to be enriched for our associated genes. For human data, these were neurons in the cortex ($P = 2.16 \times 10^{-6}$), and

GW26 GABAergic neurons in the prefrontal cortex ($P = 6.59 \times 10^{-8}$). For mouse data, these were excitatory glutamatergic neurons in cortical pyramidal layer 5 of the cerebral cortex (TEGLU10; $P = 6.98 \times 10^{-6}$) and excitatory glutamatergic/nitric oxide neurons in the tegmental reticular nucleus of the pons in the hindbrain (HBGLU8; $P = 6.74 \times 10^{-7}$). The enrichment in GABAergic neurons is interesting because there is growing evidence to suggest that impairment of the GABAergic system caused by aging results in an imbalance in the inhibitory/excitatory process involved in the neuronal response to cellular challenges and environmental changes. This results in increased vulnerability to synaptopathy and cognitive decline [39].

Gene-set analysis performed on curated gene sets and Gene Ontology (GO) [40] terms using the full distribution of SNP P-values from the *Resilience* GWAS identified two GO terms to be significantly enriched after adjustment for multiple testing. These were the biological process “neuron differentiation” ($P = 9.7 \times 10^{-07}$) and the cellular component “synaptic part” ($P = 2.14 \times 10^{-06}$). Bi-directional conditional analysis using MAGMA 1.08 [41] showed that these two annotations were independent of each other (Supplementary Table 15).

Genetic correlations with other traits

We compared our *Resilience* GWAS with recent published GWAS of cognitive phenotypes, psychiatric and neurological disorders, and global brain imaging phenotypes using LDSR analysis. *Resilience* had strong correlations with both intelligence [42] ($r_g = -0.26$, $P = 1.29 \times 10^{-17}$) and educational attainment [15] ($r_g = -0.45$, $P = 1.64 \times 10^{-56}$). These correlations are negative because our analysis used below average EY cases and above average EY controls whereas GWAS of intelligence and educational attainment report the SNP alleles associated with higher intelligence or greater educational attainment. Of the 13 independent genome-wide significant SNPs for *Resilience*, 6 are associated with intelligence at genome-wide significant levels ($P < 5 \times 10^{-8}$) but the remaining 7 SNPs are not associated with intelligence ($P > 0.01$). This indicates that some of genetic basis of *Resilience* does not overlap with the genetics of intelligence.

When psychiatric phenotypes were corrected for multiple testing ($P_{\text{bon}} = 2.4 \times 10^{-3}$), *Resilience* had a small positive correlation with unipolar depression [43] ($r_g = 0.17$, $P = 5.0 \times 10^{-10}$), a small negative correlation with schizophrenia [44] ($r_g = -0.18$, $P = 1.24 \times 10^{-12}$) and bipolar disorder [45] ($r_g = -0.17$, $P = 1.84 \times 10^{-7}$), and a nominally significant negative correlation with neuroticism [46] ($r_g = -0.07$, $P = 2.02 \times 10^{-2}$). Examination of neurological

disorders showed *Resilience* had a small nominally significant correlation with amyotrophic lateral sclerosis (ALS) [47] ($r_g = -0.21$, $P = 1.44 \times 10^{-2}$), stroke [54] ($r_g = 0.08$, $P = 1.89 \times 10^{-2}$), and Parkinson's disease [48] ($r_g = -0.08$, $P = 4.58 \times 10^{-02}$), but Alzheimer's disease (AD) [49] was not significant ($r_g = 0.04$, $P = 0.358$) (Supplementary Table 16 and Figure 5).

The GWAS of 11 brain phenotypes from the UK Biobank [50] were examined by LDSC for genetic correlation with the *Resilience* (Supplementary Table 17 and Figure 5). The volume of global white and grey matter and cerebral white matter in the left and right hemisphere were examined based on the relationship between brain volumes and cognition [51]. Volume of cerebrospinal fluid was included based of its documented association with brain atrophy [52] and the hippocampus, amygdala and nucleus accumbens were examined as moderators of cognitive function[53] [54]. After adjusting for multiple testing ($P_{\text{bon}} = 2.4 \times 10^{-3}$), the only significant correlations found were for white matter volumes where a small positive correlation was found between *Resilience* and global white matter volume ($r_g = 0.14$, $P = 1.19 \times 10^{-3}$), and the volume of cerebral white matter in the left ($r_g = 0.148$, $P = 1.74 \times 10^{-03}$) and right hemisphere ($r_g = 0.160$, $P = 7.34 \times 10^{-04}$).

The correlations of cognitive and psychiatric and neurological disorders are largely supported by gene enrichment analysis of the genes associated with *Resilience* here and previous GWAS of cognitive and psychiatric phenotypes. An analysis of published research from the GWAS catalog [55] showed that the significant SNPs found in this study were previously cited 294 times. A total of 47% of these citations were from studies of cognitive phenotypes (educational attainment, cognitive ability, maths ability and RT) and 5% were from studies of psychiatric disorders (Supplementary Table 18). In addition, when this exercise was repeated for overlapping mapped genes, we found that there was considerable overlap with these phenotypes amongst others. The most significant overlap was where 40 mapped genes in the *Resilience* analysis overlapped with the 99 reported genes for short sleep duration ($P = 2.03 \times 10^{-57}$). In a recent Mendelian randomisation study on sleep duration it was suggested that sleep duration may represent a potential causal pathway for cognition [56] and increase sleep in adults over 60 is associated with poorer cognitive function [57]. There was also a significant overlap with genes associated with extremely high intelligence [58] where 32 *Resilience* mapped genes overlapped with the 81 associated genes reported in that study ($P = 1.17 \times 10^{-45}$). Many of the overlapping genes for sleep duration and extremely high intelligence were on chromosome 3 (Supplementary Table 19).

Mendelian Randomisation:

To investigate whether genetic correlations reflected directional effects, we examined the potential credible causality of the relationship between *Resilience* and phenotypes where independent samples were available using Generalised Summary statistics-based Mendelian Randomisation [59] (GSMR) (Supplementary Table 20 and online methods). We observed a significant bidirectional causal effect of *Resilience* on schizophrenia ($b_{xy} = -0.25$, $P = 7.02 \times 10^{-9}$) and schizophrenia on *Resilience* ($b_{xy} = -0.07$, $P = 3.80 \times 10^{-7}$) indicating shared biological pathways between the two phenotypes. Indeed, hypergeometric analysis of reported genes from GWAS-catalog shows an overlap of 22 schizophrenia genes with resilience ($P = 1.19 \times 10^{-6}$) (Supplementary Table 19). By contrast, bipolar disorder and ALS did not have significant credible causality relationships with *Resilience*.

GSMR analysis was also performed using white matter volume variables and *Resilience*. To maintain independence between GWAS datasets, we used the *discovery.Resilience* GWAS that did not include UKB participants with imaging data. The low level of independent significant SNPs in the discovery GWAS did not allow for analysis of the causal effect of *Resilience* on white matter. A nominally significant causal association of white matter volume with *Resilience* was detected ($b_{xy} = 0.13$, $P = 0.049$) along with causal associations of left and right cerebral hemisphere white matter volume with *Resilience*. The association with the right hemisphere survived multiple test correction (left: $b_{xy} = 0.15$, $P = 0.005$; right: $b_{xy} = 0.17$, $P = 0.002$). There is no evidence of substantial pleiotropy in the GSMR analysis.

Discussion:

This study is the first, to our knowledge, to explore the genetic basis of cognitive resilience in a large data set. In the absence of longitudinal data, we have used proxy phenotypes to measure resilience and have combined case-control GWAS with structural equation modelling to extract genetic variants associated with *Resilience* in the UKB. We have shown the robustness of this method by confirming associations detected in a discovery sample in an independent replication sample and have successfully identified 13 independent genome-wide significant loci resulting in 371 mapped genes and 33 prioritized genes for *Resilience*. Functional analysis showed significant expression of associated genes in all brain tissues, and particularly in the frontal cortex. Significant enrichment of associated genes was also found at the cellular level in both GABAergic and glutamatergic neurons indicating an excitatory/inhibitory control in the prefrontal cortex, and within biological processes related to neuron differentiation and synaptic activity. Almost 30% of the mapped genes and over 50% of prioritized genes can be attributed to a single large locus on chromosome 3. We repeated our functional analysis of GWAS results minus this locus and found that all enrichments in tissues, cell types and biological processes previously identified remained significant.

Mapping of GWAS results identified genes that have been previously associated with cognitive decline including *STAUI*, *SEMF3A*, *IP6K1*, *MST1*, the *ATNX2/BRAP* locus, *ALDH2* and *DDX27*, where a likely functional missense variant is highly associated. Other associated genes involved with synaptic activity and neurogenesis include *BNS*, *DAG1*, *IP6K1* and *TET2*, pointing to potential targets for improvement of cognitive resilience.

Resilience is strongly correlated with RT [21], reflecting our study design that detected SNPs associated with faster than average RT or processing speed in individuals that previously showed below average EY. Decline in processing speed is strongly associated with decline in cognitive processing in older adults and had been found to be associated with cerebral small vessel disease and factors involved in the maintenance of cerebellar morphology[60]. In addition, better cognitive processing speed is also associated with larger cerebral cortex volumes (supporting our finding of a causal relationship with white matter volume), lower levels of inflammatory markers and insulin and is mediated by physical exercise [61]. Over half of our genome-wide significant loci for *Resilience* are not associated with intelligence,

indicating that factors such as reserve, compensation and maintenance may play a role over and above overall intelligence in determining cognitive resilience.

Our use of proxy phenotypes and GBS to generate a *Resilience* GWAS was in response to the limitation we faced by not having direct measurements of cognitive ability in large numbers of genotyped samples over an extended time period. This can be addressed by various biobanks that plan new data collection in the future. In addition, while the robustness of the method is demonstrated in a discovery and replication sample, it is limited to the UK Biobank and is not confirmed here in another data set.

This study demonstrated a new method to explore cognitive resilience and identifies associated loci and genes that provide neurobiological insights for this phenotype. It suggests that cognitive resilience is not just a function of superior intelligence and is causally related to variation in white matter volume. This in turn may represent a potential target for studies seeking to enhance resilience therapeutically.

Acknowledgements:

This research has been conducted using the UK Biobank Resource (project # 23739). We would like to thank all the participants and scientific researchers who contributed to the data used in this analysis. In addition we would like to acknowledge the support for data analysis provided by Declan Bennett, School of Mathematics, Statistics and Applied Mathematics, National University of Ireland, Galway.

References

1. Deary IJ, Corley J, Gow AJ, Harris SE, Houlihan LM, Marioni RE et al. Age-associated cognitive decline. *British Medical Bulletin*. 2009;92(1):135-52. doi:10.1093/bmb/ldp033.
2. Andrews SJ, Das D, Cherbuin N, Anstey KJ, Eastal S. Association of genetic risk factors with cognitive decline: the PATH through life project. *Neurobiol Aging*. 2016;41:150-8. doi:10.1016/j.neurobiolaging.2016.02.016.
3. World Health O. World report on ageing and health. Geneva: World Health Organization; 2015.
4. Staal MA, Bolton A, Yaroush R, Bourne Jr L. Cognitive performance and resilience to stress. *Biobehavioral resilience to stress*. 2008:259-99.
5. Cabeza R, Albert M, Belleville S, Craik FIM, Duarte A, Grady CL et al. Maintenance, reserve and compensation: the cognitive neuroscience of healthy ageing. *Nat Rev Neurosci*. 2018;19(11):701-10. doi:10.1038/s41583-018-0068-2.
6. Stern Y, Arenaza-Urquijo EM, Bartrés-Faz D, Belleville S, Cantilon M, Chetelat G et al. Whitepaper: Defining and investigating cognitive reserve, brain reserve, and brain maintenance. *Alzheimer's & Dementia*. 2018. doi:<https://doi.org/10.1016/j.jalz.2018.07.219>.
7. Cadar D, Robitaille A, Pattie A, Deary I, Muniz-Terrera G. The Long Arm of Childhood Intelligence on Terminal Decline: Evidence From the Lothian Birth Cohort 1921. *Psychol Aging*. 2020;35(6):806-17. doi:10.1037/pag0000477.
8. Guerra-Carrillo B, Katovich K, Bunge SA. Does higher education hone cognitive functioning and learning efficacy? Findings from a large and diverse sample. *PLOS ONE*. 2017;12(8):e0182276. doi:10.1371/journal.pone.0182276.
9. Lövdén M, Fratiglioni L, Glymour MM, Lindenberger U, Tucker-Drob EM. Education and Cognitive Functioning Across the Life Span. *Psychological Science in the Public Interest*. 2020;21(1):6-41. doi:10.1177/1529100620920576.
10. Geary DC. The Spark of Life and the Unification of Intelligence, Health, and Aging. *Current Directions in Psychological Science*. 2019;28(3):223-8. doi:10.1177/0963721419829719.

11. Sudlow C, Gallacher J, Allen N, Beral V, Burton P, Danesh J et al. UK biobank: an open access resource for identifying the causes of a wide range of complex diseases of middle and old age. *PLoS Med.* 2015;12(3):e1001779. doi:10.1371/journal.pmed.1001779.
12. Davies G, Marioni RE, Liewald DC, Hill WD, Hagenaars SP, Harris SE et al. Genome-wide association study of cognitive functions and educational attainment in UK Biobank (N=112 151). *Mol Psychiatry.* 2016;21(6):758-67. doi:10.1038/mp.2016.45.
13. Plomin R, von Stumm S. The new genetics of intelligence. *Nature Reviews Genetics.* 2018;19:148. doi:10.1038/nrg.2017.104.
14. Rietveld CA, Esko T, Davies G, Pers TH, Turley P, Benyamin B et al. Common genetic variants associated with cognitive performance identified using the proxy-phenotype method. *Proceedings of the National Academy of Sciences of the United States of America.* 2014;111(38):13790-4. doi:10.1073/pnas.1404623111.
15. Lee JJ, Wedow R, Okbay A, Kong E, Maghzian O, Zacher M et al. Gene discovery and polygenic prediction from a genome-wide association study of educational attainment in 1.1 million individuals. *Nature Genetics.* 2018;50(8):1112-21. doi:10.1038/s41588-018-0147-3.
16. Grotzinger AD, Rhemtulla M, de Vlaming R, Ritchie SJ, Mallard TT, David HW et al. Genomic structural equation modelling provides insights into the multivariate genetic architecture of complex traits. *Nature Human Behaviour.* 2019;3(5):513-25. doi:<http://dx.doi.org/10.1038/s41562-019-0566-x>.
17. Demange PA, Malanchini M, Mallard TT, Biroli P, Cox SR, Grotzinger AD et al. Investigating the genetic architecture of noncognitive skills using GWAS-by-subtraction. *Nature Genetics.* 2021;53(1):35-44. doi:10.1038/s41588-020-00754-2.
18. Watanabe K, Taskesen E, van Bochoven A, Posthuma D. Functional mapping and annotation of genetic associations with FUMA. *Nat Commun.* 2017;8(1):1826. doi:10.1038/s41467-017-01261-5.
19. Kircher M, Witten DM, Jain P, O'Roak BJ, Cooper GM, Shendure J. A general framework for estimating the relative pathogenicity of human genetic variants. *Nature Genetics.* 2014;46(3):310-5. doi:10.1038/ng.2892.
20. Benner C, Spencer CCA, Havulinna AS, Salomaa V, Ripatti S, Pirinen M. FINEMAP: efficient variable selection using summary data from genome-wide association studies. *Bioinformatics.* 2016;32(10):1493-501. doi:10.1093/bioinformatics/btw018.

21. Davies G, Lam M, Harris SE, Trampush JW, Luciano M, Hill WD et al. Study of 300,486 individuals identifies 148 independent genetic loci influencing general cognitive function. *Nat Commun.* 2018;9(1):2098. doi:10.1038/s41467-018-04362-x.
22. Tasaki S, Gaiteri C, Mostafavi S, Yu L, Wang Y, De Jager PL et al. Multi-omic Directed Networks Describe Features of Gene Regulation in Aged Brains and Expand the Set of Genes Driving Cognitive Decline. *Front Genet.* 2018;9:294-. doi:10.3389/fgene.2018.00294.
23. Annamneedi A, Caliskan G, Müller S, Montag D, Budinger E, Angenstein F et al. Ablation of the presynaptic organizer Bassoon in excitatory neurons retards dentate gyrus maturation and enhances learning performance. *Brain Struct Funct.* 2018;223(7):3423-45. doi:10.1007/s00429-018-1692-3.
24. Kim M-G, Zhang S, Park H, Park SJ, Kim S, Chung C. Inositol hexakisphosphate kinase-1 is a key mediator of prepulse inhibition and short-term fear memory. *Mol Brain.* 2020;13(1):72-. doi:10.1186/s13041-020-00615-3.
25. Wang P, Geng J, Gao J, Zhao H, Li J, Shi Y et al. Macrophage achieves self-protection against oxidative stress-induced ageing through the Mst-Nrf2 axis. *Nat Commun.* 2019;10(1):755-. doi:10.1038/s41467-019-08680-6.
26. Gontier G, Iyer M, Shea JM, Bieri G, Wheatley EG, Ramalho-Santos M et al. Tet2 Rescues Age-Related Regenerative Decline and Enhances Cognitive Function in the Adult Mouse Brain. *Cell Rep.* 2018;22(8):1974-81. doi:10.1016/j.celrep.2018.02.001.
27. Gardiner SL, Trompet S, Sabayan B, Boogaard MW, Jukema JW, Slagboom PE et al. Repeat variations in polyglutamine disease-associated genes and cognitive function in old age. *Neurobiology of Aging.* 2019;84:236.e17-.e28. doi:<https://doi.org/10.1016/j.neurobiolaging.2019.08.002>.
28. Lastres-Becker I, Nonis D, Nowock J, Auburger G. New alternative splicing variants of the ATXN2 transcript. *Neurological Research and Practice.* 2019;1(1):22. doi:10.1186/s42466-019-0025-1.
29. Timmers PR, Mounier N, Lall K, Fischer K, Ning Z, Feng X et al. Genomics of 1 million parent lifespans implicates novel pathways and common diseases and distinguishes survival chances. *Elife.* 2019;8:e39856. doi:10.7554/eLife.39856.
30. Melzer D, Pilling LC, Ferrucci L. The genetics of human ageing. *Nature Reviews Genetics.* 2020;21(2):88-101. doi:10.1038/s41576-019-0183-6.

31. Wu NN, Ren J. Aldehyde Dehydrogenase 2 (ALDH2) and Aging: Is There a Sensible Link? *Advances in experimental medicine and biology*. 2019;1193:237-53. doi:10.1007/978-981-13-6260-6_15.
32. Jackson TC, Kotermanski SE, Kochanek PM. Whole-transcriptome microarray analysis reveals regulation of Rab4 by RBM5 in neurons. *Neuroscience*. 2017;361:93-107. doi:10.1016/j.neuroscience.2017.08.014.
33. Panzanelli P, Früh S, Fritschy J-M. Differential role of GABAA receptors and neuroligin 2 for perisomatic GABAergic synapse formation in the hippocampus. *Brain Structure and Function*. 2017;222(9):4149-61. doi:10.1007/s00429-017-1462-7.
34. McLaren W, Gil L, Hunt SE, Riat HS, Ritchie GRS, Thormann A et al. The Ensembl Variant Effect Predictor. *Genome Biology*. 2016;17(1):122. doi:10.1186/s13059-016-0974-4.
35. The Genotype-Tissue Expression (GTEx) pilot analysis: Multitissue gene regulation in humans. *Science*. 2015;348(6235):648. doi:10.1126/science.1262110.
36. Zhong S, Zhang S, Fan X, Wu Q, Yan L, Dong J et al. A single-cell RNA-seq survey of the developmental landscape of the human prefrontal cortex. *Nature*. 2018;555(7697):524-8. doi:10.1038/nature25980.
37. Darmanis S, Sloan SA, Zhang Y, Enge M, Caneda C, Shuer LM et al. A survey of human brain transcriptome diversity at the single cell level. *Proceedings of the National Academy of Sciences of the United States of America*. 2015;112(23):7285-90. doi:10.1073/pnas.1507125112.
38. Zeisel A, Hochgerner H, Lönnerberg P, Johnsson A, Memic F, van der Zwan J et al. Molecular Architecture of the Mouse Nervous System. *Cell*. 2018;174(4):999-1014.e22. doi:10.1016/j.cell.2018.06.021.
39. Rozycka A, Liguz-Leczna M. The space where aging acts: focus on the GABAergic synapse. *Aging Cell*. 2017;16(4):634-43. doi:10.1111/ace1.12605.
40. Ashburner M, Ball CA, Blake JA, Botstein D, Butler H, Cherry JM et al. Gene ontology: tool for the unification of biology. The Gene Ontology Consortium. *Nature genetics*. 2000;25(1):25-9. doi:10.1038/75556.
41. de Leeuw CA, Mooij JM, Heskes T, Posthuma D. MAGMA: Generalized Gene-Set Analysis of GWAS Data. *PLOS Computational Biology*. 2015;11(4):e1004219. doi:10.1371/journal.pcbi.1004219.

42. Savage JE, Jansen PR, Stringer S, Watanabe K, Bryois J, de Leeuw CA et al. Genome-wide association meta-analysis in 269,867 individuals identifies new genetic and functional links to intelligence. *Nature Genetics*. 2018;50(7):912-9. doi:10.1038/s41588-018-0152-6.
43. Nagel M, Jansen PR, Stringer S, Watanabe K, de Leeuw CA, Bryois J et al. Meta-analysis of genome-wide association studies for neuroticism in 449,484 individuals identifies novel genetic loci and pathways. *Nature Genetics*. 2018;50(7):920-7. doi:10.1038/s41588-018-0151-7.
44. Pardiñas AF, Holmans P, Pocklington AJ, Escott-Price V, Ripke S, Carrera N et al. Common schizophrenia alleles are enriched in mutation-intolerant genes and in regions under strong background selection. *Nature genetics*. 2018;50(3):381-9. doi:10.1038/s41588-018-0059-2.
45. Stahl EA, Breen G, Forstner AJ, McQuillin A, Ripke S, Trubetskoy V et al. Genome-wide association study identifies 30 loci associated with bipolar disorder. *Nature Genetics*. 2019;51(5):793-803. doi:10.1038/s41588-019-0397-8.
46. Luciano M, Hagenaars SP, Davies G, Hill WD, Clarke T-K, Shireli M et al. Association analysis in over 329,000 individuals identifies 116 independent variants influencing neuroticism. *Nature Genetics*. 2018;50(1):6-11. doi:10.1038/s41588-017-0013-8.
47. van Rheenen W, Shatunov A, Dekker AM, McLaughlin RL, Diekstra FP, Pulit SL et al. Genome-wide association analyses identify new risk variants and the genetic architecture of amyotrophic lateral sclerosis. *Nature genetics*. 2016;48(9):1043-8. doi:10.1038/ng.3622.
48. Nalls MA, Blauwendraat C, Vallerga CL, Heilbron K, Bandres-Ciga S, Chang D et al. Identification of novel risk loci, causal insights, and heritable risk for Parkinson's disease: a meta-analysis of genome-wide association studies. *The Lancet Neurology*. 2019;18(12):1091-102. doi:10.1016/S1474-4422(19)30320-5.
49. Jansen IE, Savage JE, Watanabe K, Bryois J, Williams DM, Steinberg S et al. Genome-wide meta-analysis identifies new loci and functional pathways influencing Alzheimer's disease risk. *Nature Genetics*. 2019;51(3):404-13. doi:10.1038/s41588-018-0311-9.
50. Smith SM, Douaud G, Chen W, Hanayik T, Alfaro-Almagro F, Sharp K et al. Enhanced Brain Imaging Genetics in UK Biobank. *bioRxiv*. 2020:2020.07.27.223545. doi:10.1101/2020.07.27.223545.

51. Nave G, Jung WH, Karlsson Linnér R, Kable JW, Koellinger PD. Are Bigger Brains Smarter? Evidence From a Large-Scale Preregistered Study. *Psychol Sci.* 2019;30(1):43-54. doi:10.1177/0956797618808470.
52. Orellana C, Ferreira D, Muehlboeck JS, Mecocci P, Vellas B, Tsolaki M et al. Measuring Global Brain Atrophy with the Brain Volume/Cerebrospinal Fluid Index: Normative Values, Cut-Offs and Clinical Associations. *Neuro-degenerative diseases.* 2016;16(1-2):77-86. doi:10.1159/000442443.
53. Lisman J, Buzsáki G, Eichenbaum H, Nadel L, Ranganath C, Redish AD. Viewpoints: how the hippocampus contributes to memory, navigation and cognition. *Nat Neurosci.* 2017;20(11):1434-47. doi:10.1038/nn.4661.
54. Floresco SB. The nucleus accumbens: an interface between cognition, emotion, and action. *Annual review of psychology.* 2015;66:25-52. doi:10.1146/annurev-psych-010213-115159.
55. Buniello A, MacArthur JA L, Cerezo M, Harris LW, Hayhurst J, Malangone C et al. The NHGRI-EBI GWAS Catalog of published genome-wide association studies, targeted arrays and summary statistics 2019. *Nucleic Acids Research.* 2019;47(D1):D1005-D12. doi:10.1093/nar/gky1120.
56. Henry A, Katsoulis M, Masi S, Fatemifar G, Denaxas S, Acosta D et al. The relationship between sleep duration, cognition and dementia: a Mendelian randomization study. *Int J Epidemiol.* 2019;48(3):849-60. doi:10.1093/ije/dyz071.
57. Low DV, Wu MN, Spira AP. Sleep Duration and Cognition in a Nationally Representative Sample of U.S. Older Adults. *The American Journal of Geriatric Psychiatry.* 2019;27(12):1386-96. doi:<https://doi.org/10.1016/j.jagp.2019.07.001>.
58. Coleman JRI, Bryois J, Gaspar HA, Jansen PR, Savage JE, Skene N et al. Biological annotation of genetic loci associated with intelligence in a meta-analysis of 87,740 individuals. *Molecular psychiatry.* 2019;24(2):182-97. doi:10.1038/s41380-018-0040-6.
59. Zhu Z, Zheng Z, Zhang F, Wu Y, Trzaskowski M, Maier R et al. Causal associations between risk factors and common diseases inferred from GWAS summary data. *Nat Commun.* 2018;9(1):224. doi:10.1038/s41467-017-02317-2.
60. Eckert MA. Slowing Down: Age-Related Neurobiological Predictors of Processing Speed. *Frontiers in Neuroscience.* 2011;5:25. doi:10.3389/fnins.2011.00025.

61. Bott NT, Bettcher BM, Yokoyama JS, Frazier DT, Wynn M, Karydas A et al. Youthful Processing Speed in Older Adults: Genetic, Biological, and Behavioral Predictors of Cognitive Processing Speed Trajectories in Aging. *Frontiers in Aging Neuroscience*. 2017;9(55). doi:10.3389/fnagi.2017.00055.

Methods: (Refer to <https://github.com/joanfitz5/cog.res> for detailed analysis steps)

UK biobank:

The UK Biobank (UKB) is a data set of over half a million participants between the ages of 40 and 69, recruited from all over the UK in the period of 2006 to 2010 and had been described extensively elsewhere [11]. We obtained permission to access both the phenotypic and genetic data under project # 23739.

Genetic data: Genotypic data was collected, processed, quality controlled and imputed by UKB [62]. During our in-house quality control of the imputed data, we excluded samples with a Mahalanobis distance >6 SD from multi-mean of European Population structural analysis, removed samples with discordant sex information, chromosomal aneuploidies, high missingness/heterozygosity, retracted consent, and we excluded all related subjects using UKB-provided files on genomic relatedness. The final sample size used in this analysis was 333,664 participants.

Variants were screened by applying quality control filters (geno 0.02, MAF 0.001, info score 0.09 and HWE 0.0001) and removing duplicates resulted in 8,378,152 variants for use in our final analysis.

Phenotypic data:

Participants undertook a wide range of cognitive tests. The types of tests and the method of collection and reliability are described elsewhere [63, 64]. Analysis of cross-sectional cognitive data at time zero using IBM SPSS V24 [65] shows a moderate correlation between age and decline in performance on reaction time and a small correlation with numeric memory, pairs matching, prospective memory, and a weak correlation with fluid intelligence (Supplementary Table 21). Fluid intelligence was repeated at two subsequent intervals, however no significant sensitivity to aging was found. Deficiencies in the robustness of the longitudinal data collected at the second and third time points have been discussed elsewhere [9,10].

Generation of resilience phenotype:

Given the lack of longitudinal data, an alternative approach was to use proxy phenotypes. For past cognitive performance we examined the use of educational attainment / years in

education [13]. Educational attainment is available for 332,089 individuals in UKB that met our genotypic QC requirements. In the data set, age completed full time education was recorded for participants who did not go to college but not for those who attended higher education. We therefore assigned a default score of 20 to those who attended college and created a binary phenotype using less than or equal to age 17 to divide participants into two categories – above average and below average education years (EY). We then examined the cognitive data and selected the parameter of processing speed as measured by reaction time (RT) as an indicator of current cognitive performance. RT was chosen as it had a good correlation with age and data was available on most participants (N=331,495). RT was adjusted for age and to improve normality [12], the natural log of corrected RT was computed, and a binary RT variable was created using the mean value (5.71). Those with a value less than or equal to the mean were considered to have faster than average processing speed/RT (quicker to react) and those above the mean were considered to have slower than average processing speed/RT. At total of 330,098 individuals had measurements for EY and RT and genetic data and these made up the final sample (Supplementary Table 22).

Using these two binary variables – above or below average EY and faster or slower RT – we created four group of participants (Figure 1b). One of these groups demonstrated high resilience and these were our cases for our first “EY+Res” GWAS who had below average EY previously and faster than average RT now. A second group demonstrated low resilience or cognitive decline, and these were our controls for that GWAS who had above average EY previously and slower than average RT now. The two remaining groups of UKB samples displayed consistent cognitive performance over time. Here our cases for our second “EY/NonRes” GWAS had below average EY previously and slower than average RT now (below average cognition over time) and our controls had above average EY previously and faster than average RT now (above average cognition over time).

GWAS-by subtraction:

To extract those SNPs that were associated with resilience only we used Genomics Structural Equation Modelling (GenomicSEM) [16]. There are several processing steps that need to be performed to enable the summary statistics to be processed through GenomicSEM and these are described in the original paper by Grotzinger et al and accompanying tutorials [16, 66]. Following closely the process use by Demange et al [17], we defined a Cholesky model (Figure 2) as follows using the summary statistics from the EY+Res and EY/NonRes

GWASs. Both EY+Res and EY/NonRes were regressed on a latent factor, which captured the shared genetic variance in EY (hereafter “*EduYears*”). EY+Res was further regressed on a second latent factor capturing the variance in EY+Res independent of EY/NonRes, hereafter “*Resilience*”. Genetic variance in *Resilience* was independent of genetic variance in *EduYears* ($r_g = 0$) as the *Resilience* factor represents residual genetic variation in our EY+Res phenotype that is not accounted for by the *EduYears* factor. These two latent variables, *Resilience* and *EduYears* were then regressed on each SNP in the original GWASs (EY+Res and EY/NonRes) resulting in new GWAS summary statistics for both *Resilience* and *EduYears* (Figure 2). To calculate the path loadings for $\lambda_{\text{EduYears}} - \text{EY+Res}$ and $\lambda_{\text{Resilience}} - \text{EY+Res}$, the model was run without the SNPs.

Execution of GBS:

To show replication of our GBS-based *Resilience* GWAS, we divided the UKB into a discovery (81%) and replication (19%) sample. The replication sample included those participants in UKB that had brain imaging data available (n=37,439). Sample sizes used for analysis are shown in Supplementary Table 1. For the discovery, replication and full analysis we performed two initial GWAS for each sample (EY+Res and EY/NonRes) in plink2.0 [67] using sex, age, assessment centre, genotype array and the first 8 principle components of the population stratification analysis as supplied by the UK Biobank. We then performed GBS on both sets of samples resulting in a *discovery.Resilience* and *discovery.EduYears* GWAS, a *replication.Resilience* and a *replication.EduYears* GWAS, and later a full *Resilience* GWAS and *EduYears* GWAS.

Calculation of sample size after GBS:

Running the analysis through GBS alters the sample size and it is necessary to calculate the new value for downstream analysis. To calculate sample size or effective N (N_{eff}) of the *Resilience* GWAS for test, replication and full we followed the procedure specified in GenomicSEM[16, 68] and by Demange et al [17] (see URLs). To do this we needed to determine path loading for the models used in the three analysis as the path loading differs with different sample sizes. We trimmed our data to only include SNPs with a MAF of >0.10 and <0.40 as low and high MAF can bias the result. The output of this analysis and the calculations of sample size is in Supplementary Table 23.

Additional GWAS:

To examine the effect of GBS on EY+Res we ran two further case-control GWAS of above/below average EY and faster/slower than average age corrected RT. We mirrored the sample size used to generate EY+Res and EY/NonRes by randomly selecting 82,000 samples as cases and controls from the data set. This analysis was run in plink 2.0 [67] using sex, age, assessment centre, genotype array and the first 8 principle components of the population stratification analysis as supplied by the UKB.

Identification of genomic loci associated with resilience:

Manhattan plots of GWAS outputs from original phenotypes and GBS outputs were generated in FUMA v 1.3.6 [18] using a P-value setting of $<5 \times 10^{-8}$ for genome-wide significant SNPs. We used an LD r^2 setting of 0.6 and the 1000G phase 3 European reference panel to identify independent lead SNPs and an additional r^2 setting of 0.1 to identify lead SNPs and a maximum distance for LD blocks of 250 kb to separate findings into separate genetic loci. Conditional analysis was performed where there was more than one independent significant SNP within 1000 kb distance using --condition command in Plink 1.9 [67], which adds a SNP as a covariate in GWAS analysis.

FINEMAP [20] was used to investigate causal SNPs by analysing the relationship between the candidate GWAS SNPs generated in FUMA and LD data. LD files were generated in plink 1.9 using the --r square spaces command. Results of SNPs listed by Bayes Factor for each locus were examined as well as the configuration files generated by FINEMAP to examine for causal SNPs sets. The maximum number of SNPs in a set was fixed at 3.

Function analysis of GWAS output:

We used FUMA v 1.3.6 [18] to perform functional analysis. We used the default settings as described in the Tutorial section of the website and in previous publications [49, 42]. FUMA analysis of *Resilience* is published and can be viewed publicly in FUMA as ID:171. We used the calculated effective sample size of 111,316 (Neff) for the analysis of the *Resilience* output to examine the functional consequences of SNPs on genes, Combined Annotation Dependent Depletion (CADD) scores, chromatin states and Regulome DB analysis.

Mapping SNPs to genes:

Gene-mapping was performed in FUMA using three strategies: (a) *Positional mapping* which mapped SNPs to genes based on their genomic location within a 10 kb window of known gene boundaries. (b) *Expression quantitative trait (eQTL) mapping* which aligned cis-eQTL SNPs to genes whose expression they affected, selecting information from tissue types in 4 data sets in FUMA (PsychENCODE [69], BIOS QTL [70], Blood eQTL [71], and GTEx 8 [72]). (c) *Chromatin interaction mapping* using the 3D DNA to DNA interactions mapped SNPs to genes.

Gene-set analyses: The GENE2FUNC function within FUMA examines enrichment of mapped genes using hypergeometric tests of 9494 gene-sets from GTEx [73], MSigDB [74] and GWAS catalog [75].

MAGMA gene-based analysis:

FUMA computes a gene-based genome-wide association analysis (GWGAS) from the SNP-based P-value from the GWAS. A total of 18,879 protein coding genes containing a minimum of one GWAS SNP were used in this analysis and were used to test for association with 53 tissue types. Associations were Bonferroni corrected for multiple testing with $P < 0.05/18,879 = 2.648 \times 10^{-6}$.

We further explored the sets of associated genes in cell type specificity analyses with scRNA-seq in FUMA [76] using the following data sets: GSE104276 Human Prefrontal cortex per ages [36], GSE67835 Human Cortex [77] and Linnarsson Mouse Brain Atlas [38]. We analysed significant cell types across datasets, independent cell type associations based on within-dataset conditional analyses and pair-wise cross-datasets conditional analyses.

Comparison with published traits

LD score regression (LDSR) analysis was performed using the LDSC function within GenomicSEM [16] to examine the genetic correlation between *Resilience* with other phenotypes. Various sources were used to obtain summary statistics from GWAS of published research in psychiatry, brain imaging, and other traits of interest (supplementary Table 16 and 17). Munged summary statistic files generated during GBS were used for

Resilience, *EduYears*, *EY+Res* and *EY/NonRes* in the LDSR. Associations were Bonferroni corrected for multiple testing with $P < 0.05/21 = 2.88 \times 10^{-3}$.

Mendelian Randomisation:

Mendelian randomisation was performed using Generalized Summary statistics-based Mendelian Randomization [78] GSMR using the GCTA tool [79]. The procedure examines credible causal associations between different traits based on GWAS outputs and requires non-overlapping samples. This restricted our analysis because most of the traits examined by LDSC contained UKB participants. However the sample used for the *discovery.Resilience* GWAS (section 1.2.1) does not contain individuals that have imaging data within the UKB so we used this cohort to examine unidirectional and bidirectional causal associations between *Resilience* and phenotypes that showed significant correlations with *Resilience* using LDSC. We used a HEIDI-outlier p-value of 0.01 for outlier detection analysis. Given the low level of independent significant SNPs in the *discovery.Resilience* GWAS and the imaging GWAS, we reduced the default minimum level of significant SNPs from 10 to 8. For the disorders of ALS, bipolar disorder and schizophrenia we used the full *Resilience* GWAS and ran the analysis at the default setting of a minimum of 10. Associations were Bonferroni corrected for multiple testing with $P < 0.05/12 = 4.23 \times 10^{-3}$.

URLs:

UK Biobank: <http://biobank.ndph.ox.ac.uk>

Plink: www.cog-genomics.org/plink/2.0/

GenomicSEM: <https://github.com/MichelNivard/GenomicSEM/wiki>

GWAS-by-subtraction: <https://rpubs.com/MichelNivard/565885>

GBS sample size (N effective) calculation: https://github.com/PerlineDemange/non-cognitive/blob/master/GenomicSEM/Cholesky%20model/Calculation_samplesize.R

Functional Mapping and Annotation (FUMA): <https://fuma.ctglab.nl/downpage.html>

Venn diagram: <http://bioinformatics.psb.ugent.be/webtools/Venn/>

FINEMAP: <http://www.christianbenner.com/>

Generalised Summary-data-based MR: <https://cnsgenomics.com/software/gcta/#GSMR>

GWAS Catalog: <https://www.ebi.ac.uk/gwas/>

GWAS Atlas: <https://atlas.ctglab.nl/>

Ensembl Variant Effect Predictor: <https://www.ensembl.org/Tools/VEP>

References

11. Sudlow C, Gallacher J, Allen N, Beral V, Burton P, Danesh J et al. UK biobank: an open access resource for identifying the causes of a wide range of complex diseases of middle and old age. *PLoS Med.* 2015;12(3):e1001779. doi:10.1371/journal.pmed.1001779.
12. Davies G, Marioni RE, Liewald DC, Hill WD, Hagenaars SP, Harris SE et al. Genome-wide association study of cognitive functions and educational attainment in UK Biobank (N=112 151). *Mol Psychiatry.* 2016;21(6):758-67. doi:10.1038/mp.2016.45.
16. Grotzinger AD, Rhemtulla M, de Vlaming R, Ritchie SJ, Mallard TT, David HW et al. Genomic structural equation modelling provides insights into the multivariate genetic architecture of complex traits. *Nature Human Behaviour.* 2019;3(5):513-25. doi:<http://dx.doi.org/10.1038/s41562-019-0566-x>.
17. Demange PA, Malanchini M, Mallard TT, Biroli P, Cox SR, Grotzinger AD et al. Investigating the genetic architecture of noncognitive skills using GWAS-by-subtraction. *Nature Genetics.* 2021;53(1):35-44. doi:10.1038/s41588-020-00754-2.
18. Watanabe K, Taskesen E, van Bochoven A, Posthuma D. Functional mapping and annotation of genetic associations with FUMA. *Nat Commun.* 2017;8(1):1826. doi:10.1038/s41467-017-01261-5.
20. Benner C, Spencer CCA, Havulinna AS, Salomaa V, Ripatti S, Pirinen M. FINEMAP: efficient variable selection using summary data from genome-wide association studies. *Bioinformatics.* 2016;32(10):1493-501. doi:10.1093/bioinformatics/btw018.
36. Zhong S, Zhang S, Fan X, Wu Q, Yan L, Dong J et al. A single-cell RNA-seq survey of the developmental landscape of the human prefrontal cortex. *Nature.* 2018;555(7697):524-8. doi:10.1038/nature25980.
38. Zeisel A, Hochgerner H, Lönnerberg P, Johnsson A, Memic F, van der Zwan J et al. Molecular Architecture of the Mouse Nervous System. *Cell.* 2018;174(4):999-1014.e22. doi:10.1016/j.cell.2018.06.021.
42. Savage JE, Jansen PR, Stringer S, Watanabe K, Bryois J, de Leeuw CA et al. Genome-wide association meta-analysis in 269,867 individuals identifies new genetic and functional links to intelligence. *Nature Genetics.* 2018;50(7):912-9. doi:10.1038/s41588-018-0152-6.

49. Jansen IE, Savage JE, Watanabe K, Bryois J, Williams DM, Steinberg S et al. Genome-wide meta-analysis identifies new loci and functional pathways influencing Alzheimer's disease risk. *Nature Genetics*. 2019;51(3):404-13. doi:10.1038/s41588-018-0311-9.
62. Bycroft C, Freeman C, Petkova D, Band G, Elliott LT, Sharp K et al. The UK Biobank resource with deep phenotyping and genomic data. *Nature*. 2018;562(7726):203-9. doi:10.1038/s41586-018-0579-z.
63. Lyall DM, Cullen B, Allerhand M, Smith DJ, Mackay D, Evans J et al. Cognitive Test Scores in UK Biobank: Data Reduction in 480,416 Participants and Longitudinal Stability in 20,346 Participants. *PLoS One*. 2016;11(4):e0154222. doi:10.1371/journal.pone.0154222.
64. Fawns-Ritchie C, Deary IJ. Reliability and validity of the UK Biobank cognitive tests. *PloS one*. 2020;15(4):e0231627-e. doi:10.1371/journal.pone.0231627.
65. IBM Corp. Released 2016. IBM SPSS Statistics for Windows VA, NY: IBM Corp.
66. Nivard M. GenomicSem. 2019. <https://github.com/MichelNivard/GenomicSEM/wiki>.
67. Chang CC, Chow CC, Tellier LCAM, Vattikuti S, Purcell SM, Lee JJ. Second-generation PLINK: rising to the challenge of larger and richer datasets. *GigaScience*. 2015;4(1). doi:10.1186/s13742-015-0047-8.
68. Mallard TT, Linnér RK, Grotzinger AD, Sanchez-Roige S, Seidlitz J, Okbay A et al. Multivariate GWAS of psychiatric disorders and their cardinal symptoms reveal two dimensions of cross-cutting genetic liabilities. *bioRxiv*. 2020:603134. doi:10.1101/603134.
69. Wang D, Liu S, Warrell J, Won H, Shi X, Navarro FCP et al. Comprehensive functional genomic resource and integrative model for the human brain. *Science*. 2018;362(6420). doi:10.1126/science.aat8464.
70. Bonder MJ, Luijk R, Zhernakova DV, Moed M, Deelen P, Vermaat M et al. Disease variants alter transcription factor levels and methylation of their binding sites. *Nature Genetics*. 2017;49(1):131-8. doi:10.1038/ng.3721.
71. Westra H-J, Peters MJ, Esko T, Yaghootkar H, Schurmann C, Kettunen J et al. Systematic identification of trans eQTLs as putative drivers of known disease associations. *Nature Genetics*. 2013;45(10):1238-43. doi:10.1038/ng.2756.
72. Battle A, Brown CD, Engelhardt BE, Montgomery SB. Genetic effects on gene expression across human tissues. *Nature*. 2017;550(7675):204-13. doi:10.1038/nature24277.

73. A Novel Approach to High-Quality Postmortem Tissue Procurement: The GTEx Project. *Biopreservation and Biobanking*. 2015;13(5):311-9. doi:10.1089/bio.2015.0032.
74. Liberzon A, Birger C, Thorvaldsdóttir H, Ghandi M, Mesirov JP, Tamayo P. The Molecular Signatures Database (MSigDB) hallmark gene set collection. *Cell Syst*. 2015;1(6):417-25. doi:10.1016/j.cels.2015.12.004.
75. Buniello A, MacArthur JAL, Cerezo M, Harris LW, Hayhurst J, Malangone C et al. The NHGRI-EBI GWAS Catalog of published genome-wide association studies, targeted arrays and summary statistics 2019. *Nucleic Acids Res*. 2019;47(D1):D1005-d12. doi:10.1093/nar/gky1120.
76. Watanabe K, Umičević Mirkov M, de Leeuw CA, van den Heuvel MP, Posthuma D. Genetic mapping of cell type specificity for complex traits. *Nat Commun*. 2019;10(1):3222. doi:10.1038/s41467-019-11181-1.
77. Darmanis S, Sloan SA, Zhang Y, Enge M, Caneda C, Shuer LM et al. A survey of human brain transcriptome diversity at the single cell level. *Proceedings of the National Academy of Sciences*. 2015;112(23):7285. doi:10.1073/pnas.1507125112.
78. Zhu Z, Zheng Z, Zhang F, Wu Y, Trzaskowski M, Maier R et al. Causal associations between risk factors and common diseases inferred from GWAS summary data. *Nat Commun*. 2018;9(1):224. doi:10.1038/s41467-017-02317-2.
79. Yang J, Lee SH, Goddard ME, Visscher PM. GCTA: a tool for genome-wide complex trait analysis. *American journal of human genetics*. 2011;88(1):76-82. doi:10.1016/j.ajhg.2010.11.011.

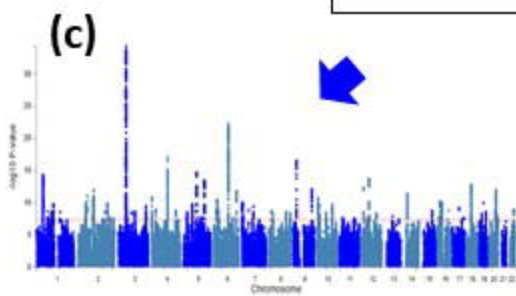
(a)

UKB Sample	
Discovery	(n=266,543; 81%)
Replication	(n=63,554; 19%)
Full	(n=330,097; 100%)

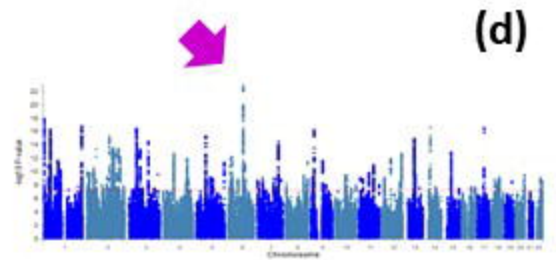
bioRxiv preprint doi: <https://doi.org/10.1101/2021.01.22.427640>; this version posted January 22, 2021. The copyright holder for this preprint (which was not certified by peer review) is the author/funder. All rights reserved. No reuse allowed without permission.

(b)

	Faster than average RT	Slower than average RT
Above average EY	EY/NonRes Controls	EY+RES Controls
Below average EY	EY+RES Cases	EY/NonRes Cases

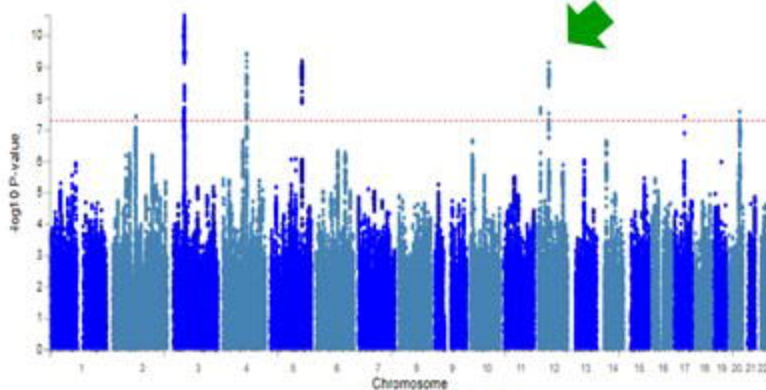


EY+Res

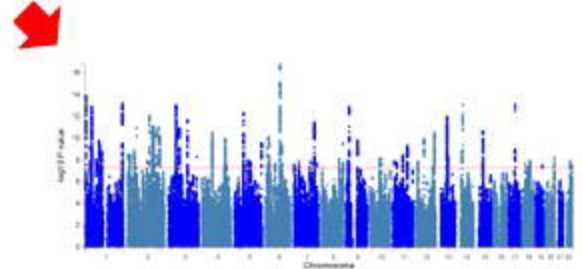


EY/NonRes

(e) GWAS-by-subtraction (GBS)
EY+Res minus EY/NonRes



Resilience



EduYears

(f)



Functional analysis

- Description of genetic loci
- Fine mapping of loci
- Gene mapping
- Tissue, cell type and pathway enrichment analysis
- Genetic correlations with other traits
- Mendelian randomisation

Figure 1: Flow chart of study design. (a) The available UKB samples were split into Discovery (81%) and Replication (19%) samples. Following successful replication analysis, the Full sample was also put through the analysis pipeline. (b) For Discovery, Replication or Full, samples were assigned to one of four categories based on their EY and RT measures. (c) EY+Res cases and controls were analysed in a GWAS. (d) EY/NonRes cases and controls were analysed in a GWAS. (e) GBS used to subtract the genetic signals for EY/NonRes from EY+Res to result in a Resilience GWAS and an EduYears GWAS. (f) Resilience GWAS functionally analysed to identify associated SNPs and genes, and enriched tissues, cell types and pathways, identify genetic correlations with other traits and explore causal relationships between resilience and other traits using Mendelian randomisation.

bioRxiv preprint doi: <https://doi.org/10.1101/2021.01.22.427640>; this version posted January 22, 2021. The copyright holder for this preprint (which was not certified by peer review) is the author/funder. All rights reserved. No reuse allowed without permission.

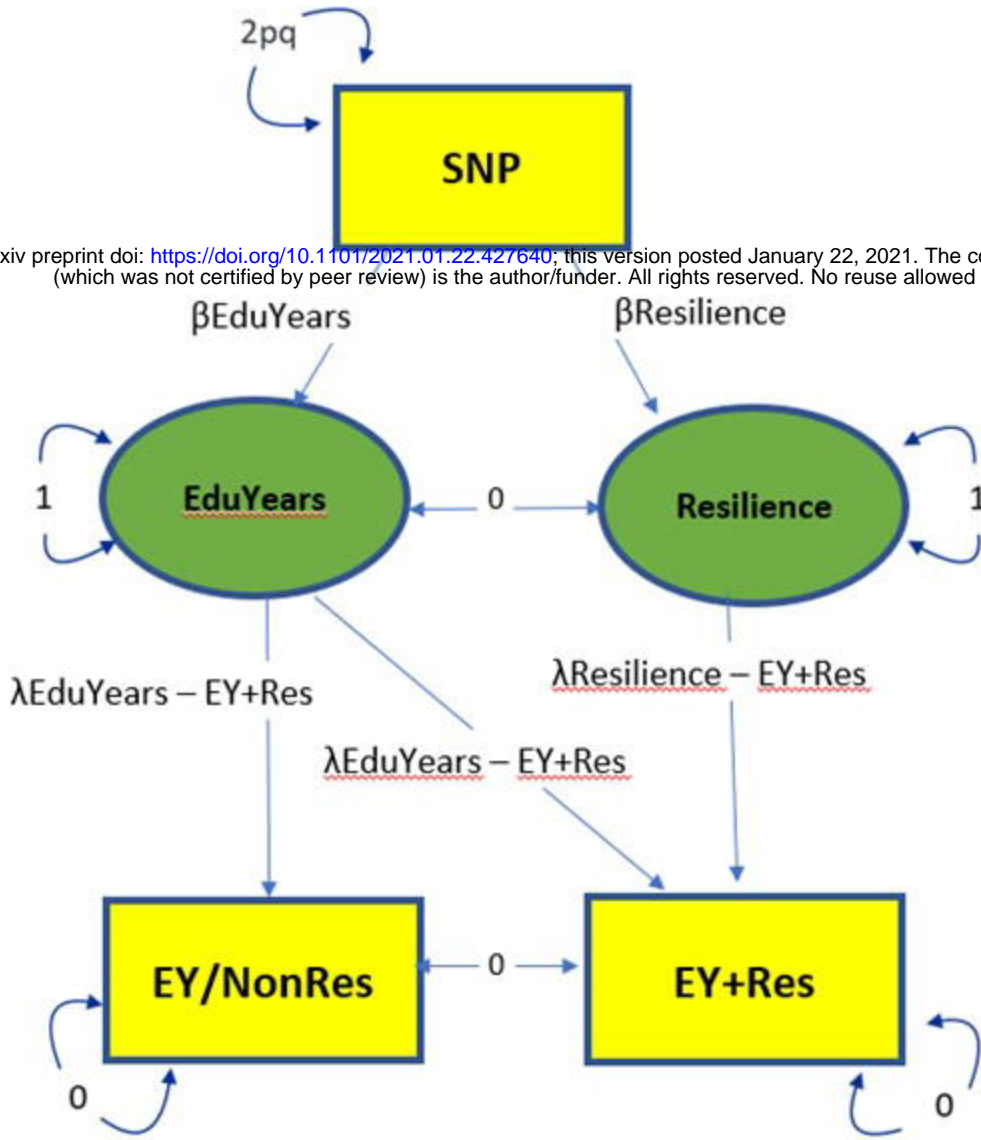
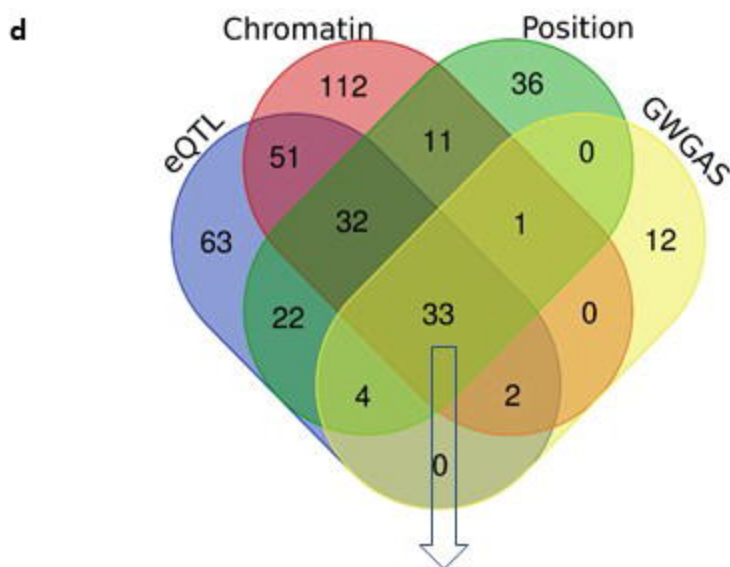
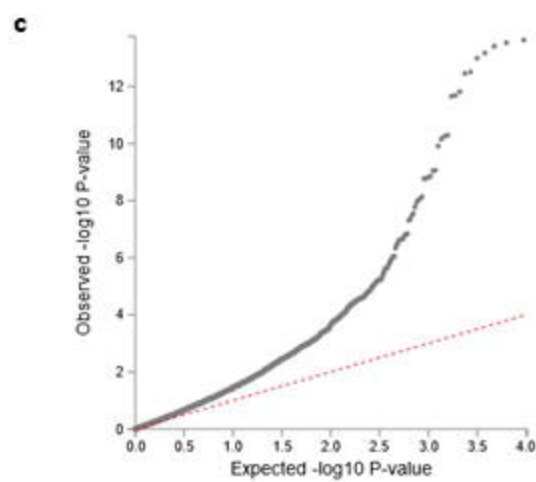
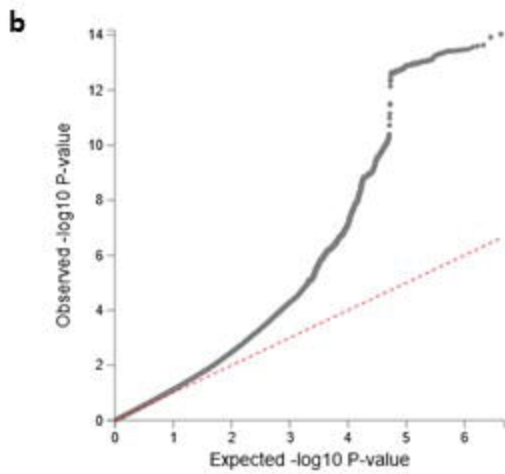
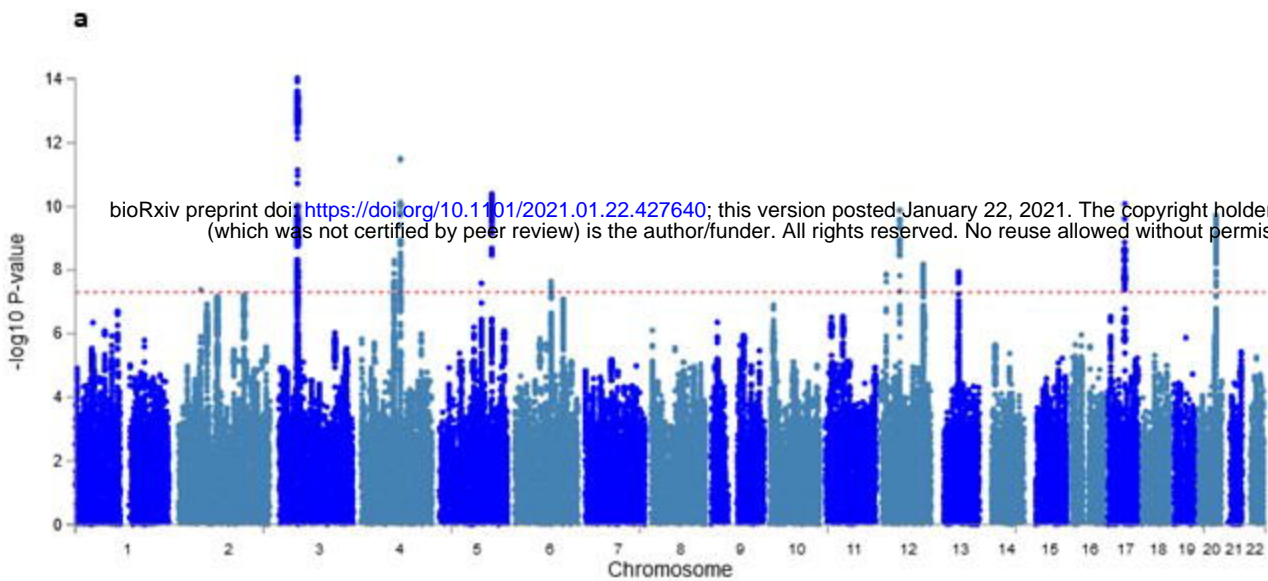


Figure 2: SEM of GWAS-by subtraction model. The observed variables are the GWAS EY+Res and EY/NonRes and SNP and the latent variables (unknown) are *Resilience* and *EduYears*. There are two pathways for the SNPs analysis in this model to EY+Res – the first is through *EduYears* to EY+Res and EY/NonRes and incorporates the genetic effects of the variables used in the phenotype. The other path is through *Resilience* to EY+Res and measures the genetic effect of resilience independent of *EduYears*. To calculate the model, the genetic covariances between EY+Res and EY/NonRes and *Resilience* and *EduYears* are set to 0 and the variances of EY+Res and EY/NonRes are also set to 0. The variance is therefore explained by the latent factors. The SNP value is calculated as $2pq$ from allele frequencies of the 1000 Genome phase 3 data where p is the reference allele and q the alternative allele.



ACAD10, ALDH2, AMT, ATXN2, BRAP, BSN, CAMKV, CSE1L, CTD-2330K9.3, MAPKAPK5, MON1A, CYSTM1, DAG1, DDN, GNAT1, GPX, IP6K1, MST1, RBM5, RHOA, RNF123, MST1R, NICN1, PFDN1, PRKAG1, SEMA3F, SH2B3, STAU1, TCTA, TET2, TMEM116, TRAIP, UBA7,

Figure 3: Resilience GWAS and gene identification. **a** Manhattan plot of *Resilience* identifying 13 independent genome-wide significant loci. **b** Quantile – quantile plot of GWAS SNPs. **c** Quantile – quantile plot of the gene-based association test. **d** Venn diagram of overlapping mapped genes by four strategies showing 33 genes were mapped by all four strategies. These genes are listed underneath.

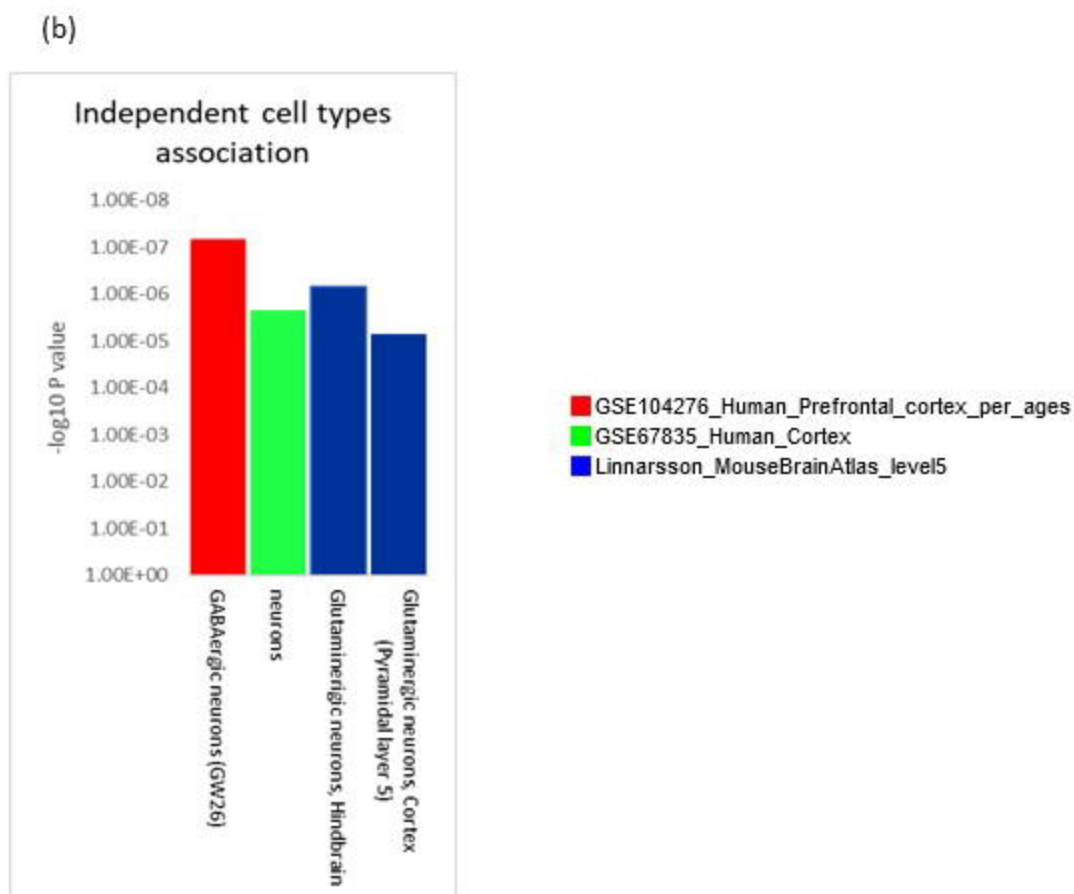
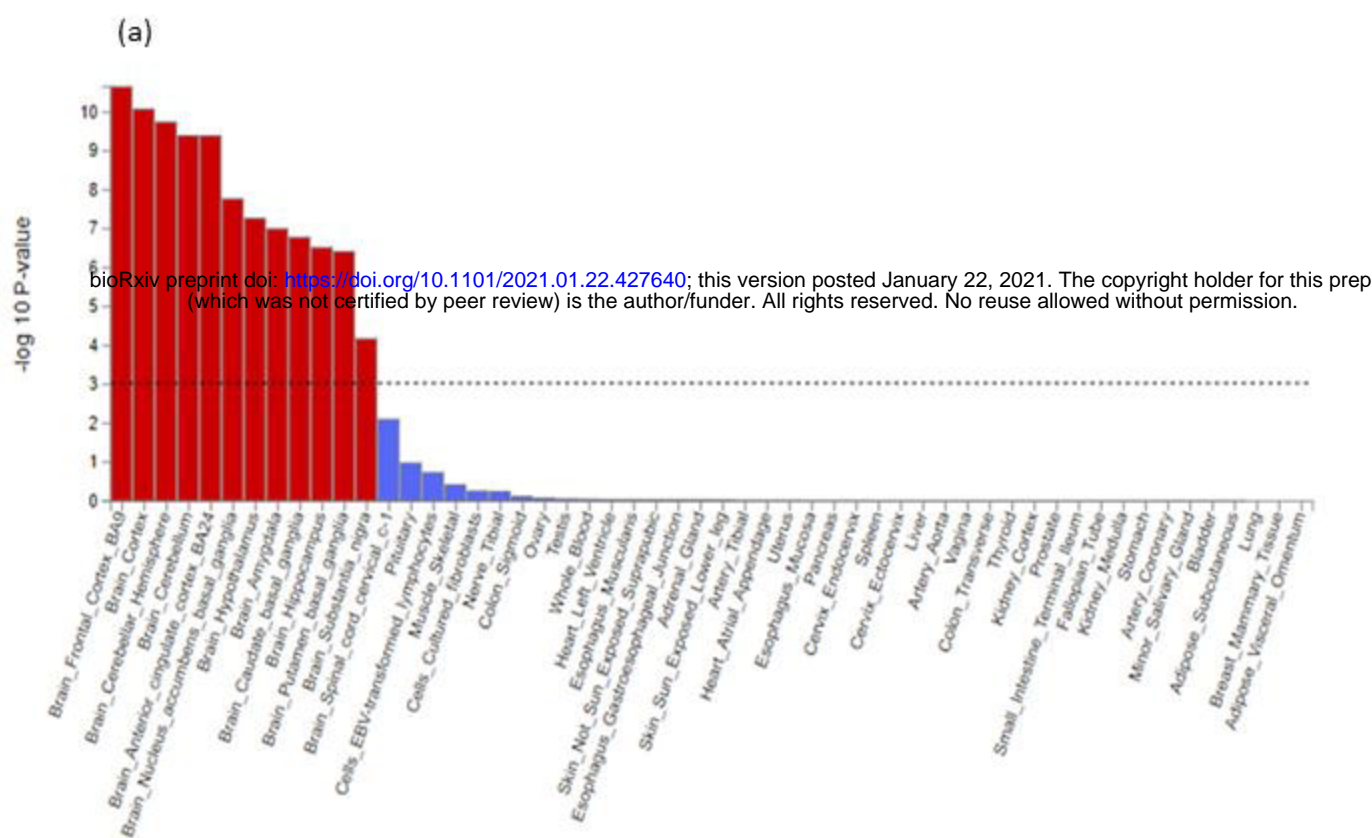


Figure 4: (a) Gene - tissue expression analysis based on GTEx RNA-seq data (b) Independent cell type associations based on within-dataset conditional analyses

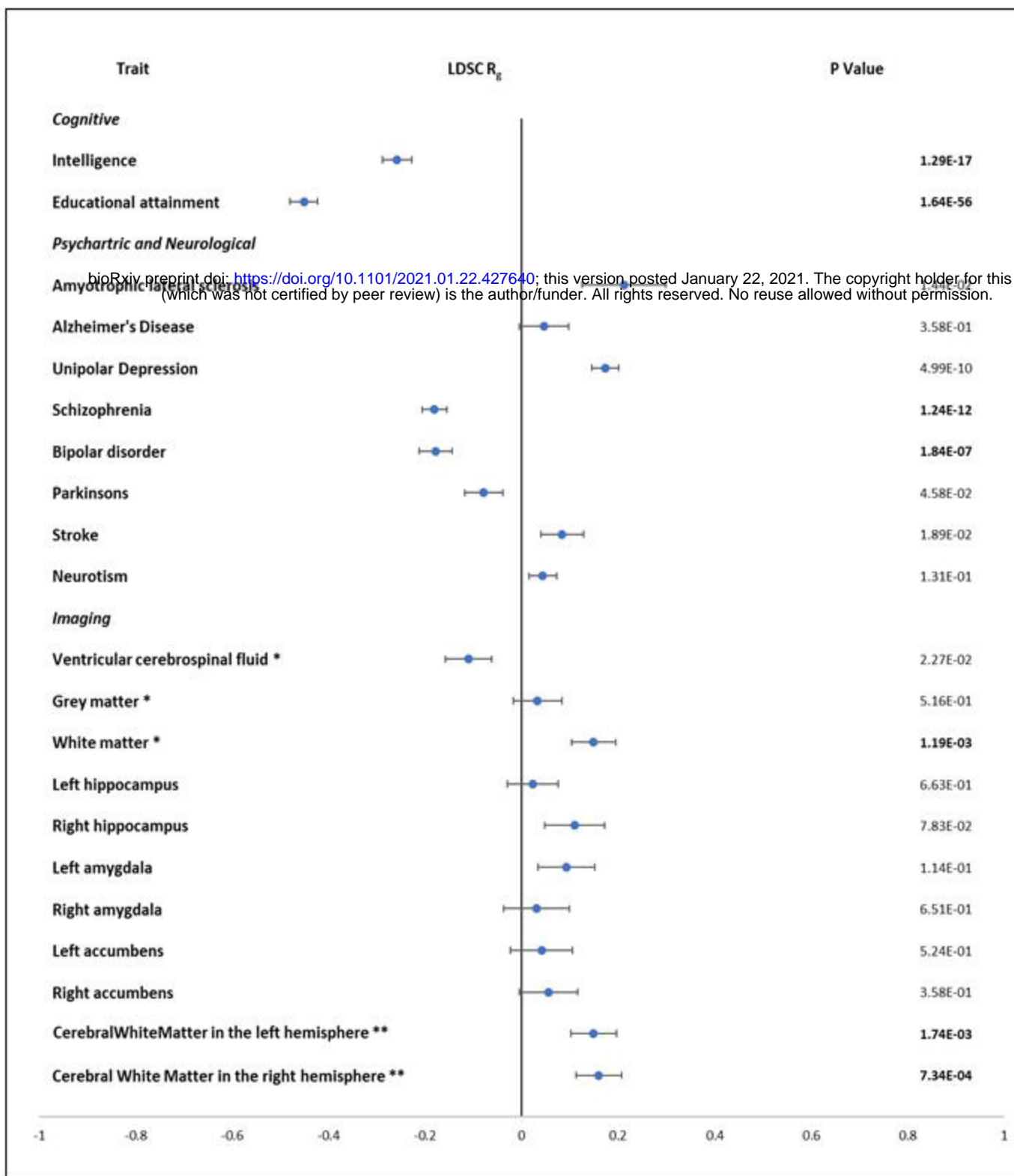


Figure 5: Genetic correlation with cognitive traits , psychiatric and brain disorders and brain imaging, significant P values corrected for multiple testing are in bold.

*normalised for head size , **generated by subcortical volumetric segmentation .